MEASURED LOADING RESPONSE OF MODEL MOTION CONTROL STERN TABS

J Bell, T Arnold, J Lavroff, M R Davis, University of Tasmania, Australia

SUMMARY

Active trim tabs are commonly used as part of the ride control systems of high-speed craft. This paper investigates the lift characteristics of rectangular stern tabs that are commonly fitted to INCAT wave-piercer catamarans. A test apparatus was developed to enable the testing of a model scale trim tab in a circulating water tunnel in the University of Tasmania hydraulics laboratory. The magnitude and location of the lift force produced by the tab were measured over a range of tab angles and flow velocities. From this the lift coefficient of the tab was calculated and the performance of the tab under varying conditions was analysed. The lift force produced by the tab was shown to increase with velocity and tab angle as expected, with the lift coefficient of the tab increasing linearly with tab angle and remaining relatively constant with increases in flow velocity. The magnitude of the measured lift coefficient was lower than had been previously estimated in shallow water tests and the force was found to act forward of the tab hinge, indicating that much of the lift force generated by the tab is due to the increased pressure on the underside of the hull forward of the tab.

NOMENCLATURE

A	Trim tab area (m^2)
α	Trim tab angle below horizontal (rad)
b	Width of elastic link cross section (m)
C_L	Trim tab lift coefficient
E	Young's Modulus of aluminium (N m^{-2})
F	Trim tab lift force (N)
GF	Strain gauge factor
h	Height of elastic link cross section (m)
I	Second moment of area of elastic link (m^4)
l_1	Distance of aft elastic link to tab hinge (m)
l_2	Distance of forward elastic link to tab hinge (m)
M_A	Bending moment about aft elastic link (Nm)
M_F	Bending moment about forward elastic link (Nm)
Q	Volumetric flow rate (m^3s^{-1})
R	Strain bridge resistance (Ω)
V	Flow velocity (m s^{-1})
V_{ex}	Strain bridge excitation voltage (V)
V_o	Strain bridge output voltage (V)
x	Distance of lift force effective location to tab hinge (m)
y	Distance from neutral axis of elastic link to strain gauge mounting surface (m)
ε	Strain measured in elastic links
σ	Bending stress in elastic links (N m^{-2})
ρ	Density of water (kg m^{-3})

1. INTRODUCTION

The increasing focus on speed and efficiency in sea transportation has led to the development of large high-speed catamarans capable of carrying higher loads at increased speeds. High-speed catamarans such as those manufactured by INCAT Tasmania are commonly used by ferry services due to their high speed, stability, large deck area and high payload to ship weight ratio. These properties have also seen the use of high-speed catamarans extend to military transportation roles. In order to provide a competitive transport option, ship builders are increasingly looking to maximise the payload to ship weight ratio, whilst also providing a vessel which can continue operating at high speeds in more severe sea conditions. Due to the catamaran design, with widely spaced long, slender hulls, high motion accelerations and large heave and pitch motions are experienced in heavy seas as a consequence of the high operating Froude number.

The largest forces experienced by catamarans occur during slamming events [1], with potentially damaging forces exerted on the ship structure and a vibratory response through the structure known as whipping [2]. Extensive research has been done into the slamming and whipping response of high speed catamarans during both full scale sea trials [3, 4] and controlled model testing [5, 6, 7]. Ship motions have also been measured in order to determine the response to various sea conditions [8] and the effectiveness of ride controls in reducing motions and loads [9]. Ship motions contribute substantially to wave loading and slamming as well as giving rise to passenger discomfort and motion sickness [10]. Reduction of motions through the use of ride control systems is therefore considered essential. In addition to the sea trials and model testing, loads and motions are predicted numerically. This is generally done with the use of finite element software for determining loads and the sea keeping code BEAMSEA [11] for determining motions.

INCAT catamarans use a centre bow design to dampen pitching motions and reduce the occurrence and severity of slam events and deck diving in following seas. Active motion control systems are fitted to INCAT catamarans, consisting of a pair of stern mounted trim tabs and a retractable T-foil which is mounted within the aft end of the centre bow. The trim tabs work to keep the vessel on a level trim and reduce rolling and pitch motions by generating a controlled unsteady lift force at the transom of the ship. Full scale testing has shown the motion control system to be effective in damping the vessel motions and reducing the occurrence of slam events, with increased performance at higher speeds due to an

increase in the lift force generated [9]. In these sea trials the T-foil was both immersed and retracted, the tabs remaining active at all times, meaning that comparisons with and without the use of the tabs could not be made. While the effect of ride controls on the motions and loads of the ship can be determined during sea trials, the effect of motion controls has not so far been included in model testing. Also there is presently little information available on the magnitude of the forces generated by the stern tabs in different conditions of speed and tab angle, and therefore there is uncertainty regarding the effect of stern tabs in controlling motion damping and the structural loads.

A 2.5m hydroelastic segmented model of the 112m INCAT wave piercer catamaran [6] used for model tests does not currently include an active ride control system as fitted to the full scale vessel. The model does include adjustable trim tabs but they are statically mounted and no T-foil is currently fitted. A model scale T-foil has been developed and plans are currently in place to have this fitted to the model, with the intention of fitting a complete model scale active ride control system, allowing the effect of ride controls on motions and loads to be evaluated at model scale under more controlled conditions than is possible in sea trials. An improved knowledge of motion control load responses, in conjunction with model scale motions and loads data, full scale sea trials data and numerical computations will assist in the optimisation of motion control system algorithms and numerical predictions of ship motions and loads, leading to improved ship motions and reduced structural loads.

This present paper investigates the magnitude and location of the force produced by a trim tab, and thus the variation of lift coefficient of the tab at model scale for application to the INCAT 112m catamaran model [6]. The model tab and aft end of the hull underside are mounted on a pair of parallel cantilever beams which have small rectangular elastic links fitted at two locations with strain gauge pairs on top and bottom surfaces of the rectangular link. This makes possible the direct measurement of bending moment in the cantilever mounting beams at two positions, thereby facilitating the determination of the upward force on the tab and on the hull aft section and its location.

2. TEST APPARATUS

Testing was carried out in a closed circuit circulating water tunnel in the University of Tasmania Hydraulics Laboratory. The circulating water tunnel working section has a length of 1000 mm, a width of 600 mm and a usable depth of 200 mm. When operated with an open test section, the water tunnel could not achieve velocities above 1.2 m/s before the flow quality became unacceptable due to surging. Subsequently, a significant increase of velocity was produced in the flow. The required flow velocities were achieved in the water tunnel using a flow constriction flap as shown in Figure 1. The constriction flap consisted of two Perspex sheets joined together along their edges using a piano hinge. One sheet was clamped to the upstream face of the water tunnel working section and the other sheet protruded into the flow at a fixed angle. The angle of the flap was set using two vertical rods which were clamped to the frame edges on each side. The rods were allowed to slide through the clamps when they were loosened, enabling the flap to be fixed at various angles. The constriction flap reduced the cross-sectional area of the flow, which accelerated the water through the test section to achieve the required flow rates and flow velocities.

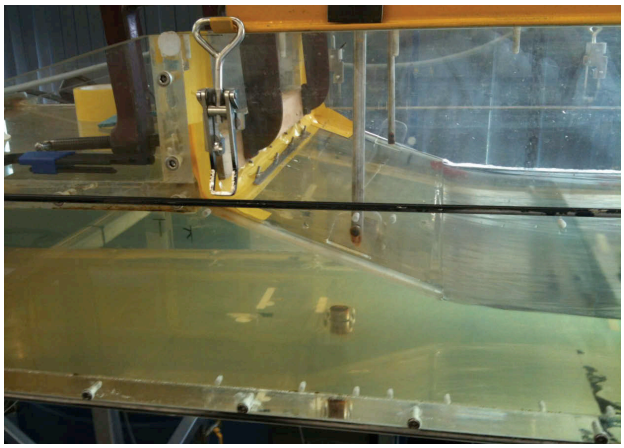

Figure 1: Circulating water tunnel flow constriction flap.

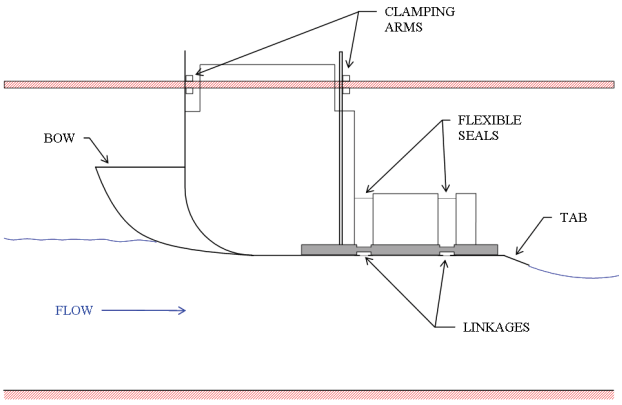

Figure 2: Schematic of experimental setup.

The test apparatus was located in the test section of the circulating water tunnel behind the constriction flap and in effect consisted of a segmented hull with a stern tab as shown in Figure 2. The horizontal base is segmented with two longitudinal connecting beams, allowing the resultant tab force to be transferred through the two longitudinal beams in which the applied strain is measured on top and bottom surfaces of the connecting links so as to indicate the bending moment at the segment joins. The design was largely dictated by the size of the circulating water tunnel test section, the maximum flow rate available and the requirement that the tab is at the scale of the hydroelastic segmented model of the 112m INCAT catamaran [6].

This design allows the magnitude and location of the tab force to be determined through measuring the bending moment induced at the forward and aft link locations. Equations (1) and (2) are the forward and aft moment equations which can easily be solved to determine the force *F*, and its location *x*:

$$M_F = F(x + l_1 + l_2) \quad (1)$$
$$M_A = F(x + l_1) \quad (2)$$

The apparatus was mostly constructed from aluminium, with a fibreglass bow section joined to the fixed forward section and two equal length aft horizontal sections, fixed together by the longitudinal beams. The width of the apparatus is 195 mm to allow adequate clearance between the circulating water tunnel walls and the segmented hull sections. A frame with mounting bars was fixed to the top of the circulating water tunnel test section, this enabling the apparatus to be secured at the forward vertical face and to a vertical support at the aft end of the rigid base segment. These bars can be attached to the apparatus at various heights so as to provide a means of raising or lowering the apparatus relative to the base of the circulating water tunnel test section. Small perspex vertical walls were mounted on the sides of the cantilever plate segments to prevent flooding over the horizontal segment plates and the gaps between the segments were sealed with latex and waterproof tape, both on the underside of the apparatus and between the wall sections. Figure 3 shows the design of the test apparatus. Table 1 gives the key dimensions of the completed apparatus as needed for calculations.

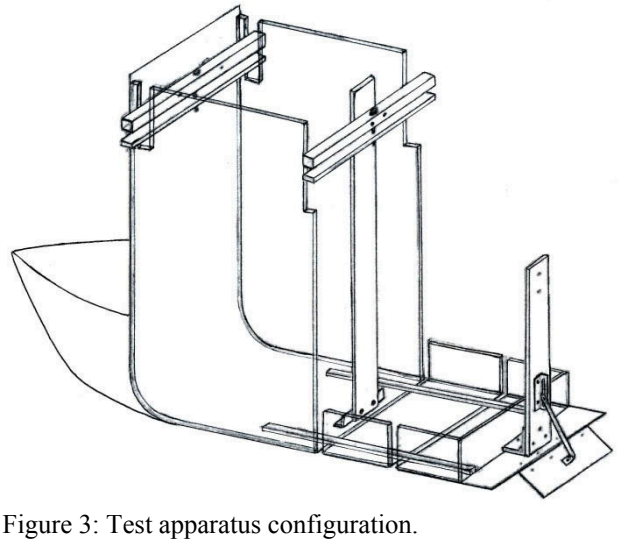

Figure 3: Test apparatus configuration.

Turbulence stimulation on the underside of the apparatus was considered, as turbulence stimulation of the boundary layer is recommended in model testing [12]. This was not implemented however, due to the positioning of the water jet intakes just forward of the trim tab on the INCAT vessel. The water jet intakes [13] are expected to significantly reduce the boundary layer aft of the intakes. The effect of the intakes on the boundary layer state would therefore need to be investigated further before any informed predictions could be made on the boundary layer state at the tab location.

Table 1: Apparatus key dimensions

Elastic Links			
	b (m)	*h* (m)	I_x (m^4)
Forward Left	0.00801	0.0048	7.382E-11
Forward Right	0.00803	0.00481	7.447E-11
Aft Left	0.0081	0.00342	2.700E-11
Aft Right	0.00792	0.00342	2.640E-11
Trim Tab Dimensions			
Effective Length (hinge centre to trailing edge) (m)			0.037
Tab Width (m)			0.130
Lever Arms			
l_1(m)			0.12
l_2(m)			0.245

Strain gauges mounted on the top and bottom of the four elastic links measure the applied strain at two distances from the tab. The strain gauges are mounted in bending pairs on machined flexible links, sized as in table 1 to allow good resolution for the estimated expected loads. A half bridge wiring configuration was used, with strain output amplified and recorded as an output voltage to a PC via a LABVIEW data acquisition program.

The bridge output voltage is given by equation (3), with the indicated strain then being given by equation (4):

$$V_0 = \left(\frac{R_4}{R_3+R_4} - \frac{R_2}{R_1+R_2}\right) V_{ex} \quad (3)$$
$$\varepsilon = \frac{-2V_o}{V_{ex}GF} \quad (4)$$

where V_o is the output voltage, V_{ex} is the bridge excitation voltage, *GF* is the gauge factor R_2 and R_4 are the strain gauge resistances and R_1 and R_2 are the other bridge resistances (all approximately 120 ohm).

The surface bending stress σ, is given from simple beam theory by equation (5) where *y* is the distance from the section centroid to the surface of the link and can be rearranged to give equations (6) and (7) to provide a measured bending moment *M*, from the measured strains at both link locations: the link second moment of area *I* takes into account both longitudinal beams:

$$\sigma = \frac{My}{I} \quad (5)$$
$$bh^2 = \frac{6M}{E\varepsilon} \quad (6)$$
$$M = \frac{bh^2E\varepsilon}{6} \quad (7)$$

Equations (1) and (2) then yield equations (8) and (9) which give the force magnitude F, and location x, relative to the tab hinge:

$$F = \frac{(M_F - M_A)}{(l_2)} \quad (8)$$

$$x = \frac{M_A}{F} - l_1 \quad (9)$$

3. CALIBRATION

Bench top deadweight calibration was carried out to determine the measured strains for known loads. The apparatus was placed upside down on a bench top, with the base of the apparatus horizontal, allowing the applied load to act in the same direction as the loads experienced during testing.

Strain from the output voltage and the applied bending moments about the forward and aft link locations were calculated as described previously. The value of I used is the sum of the second moments of area for the forward or aft links on both longitudinal beams, as the load is shared between the beams. The net upward force and its location was then calculated from the moments measured at the forward and aft link locations. The measured load was then plotted against the known applied load. Figure 4 shows the results from dead weight testing. It can be seen that the measured forces deviate from the applied forces by a small constant factor over the range of the applied loads. During this test the seals were fitted so the latex was not in tension under load: thus the seals did not have a measurable effect on readings. This was done so that during testing the self-weight of the apparatus would not act to apply tension in the seals. The calibration factor determined from Figure 4 will thus account for any differences between the actual and assumed Young's Modulus of aluminium, minor errors in link dimensions and bridge setup errors.

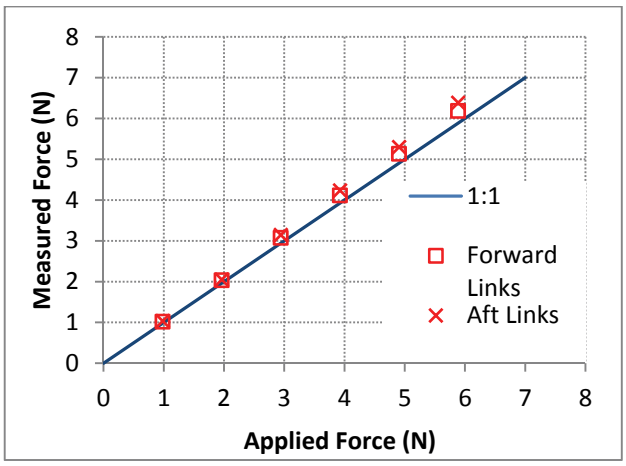

Figure 4: Dead weight calibration.

4. TESTING

The flow velocity in the test section of the circulating water tunnel was measured by means of a pitot probe located in the free stream flow between the apparatus and the bottom of the test section (Figure 5). The pitot pressure was compared with a static pressure tapping on the base of the working section to determine the flow velocity using the Bernoulli equation. Pressure measurement was performed based on a sampling rate of 1000 Hz using a Validyne DP15 variable reluctance differential pressure transducer. Based on this set-up configuration, tests were undertaken on the apparatus for tab angles of -7°, 0°, 5°, 10°, 15° and 20° over a range of flow velocities up to the maximum attainable flow velocity in the circulating water tunnel.

The strain data was recorded to a PC and was displayed graphically as output voltage against time for each of the four strain bridges and was saved in Microsoft Excel format. From the time averaged recorded voltages, the strain, stress and bending moment applied to each link could be calculated, allowing the applied force position and magnitude to be determined for each tab angle/flow velocity combination.

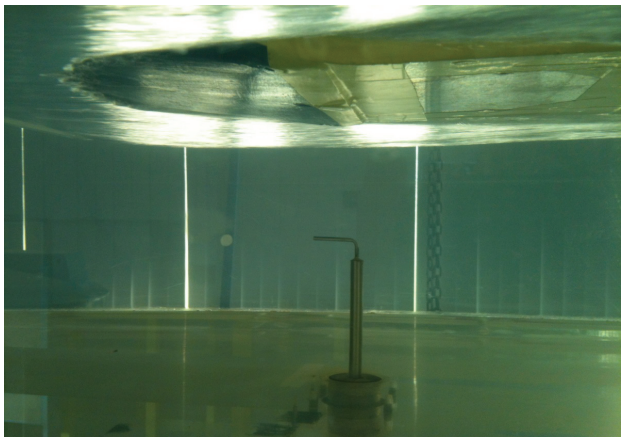

Figure 5: Pitot probe in flow under apparatus.

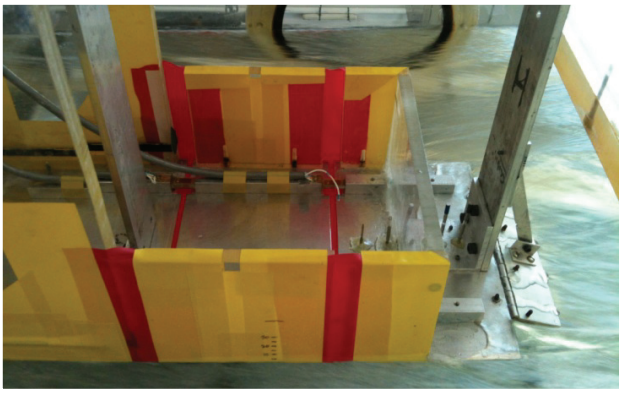

Figure 6: Detail of tab during testing.

Prior to testing, the output voltage from each strain gauge pair was zeroed with the model in place but with no flow and the sampling rate was set to 10 Hz in a LABVIEW

data acquisition program. At each tab angle measurements were made over a range of flow velocities by varying the flow rate delivered by the pump. Figure 6 shows a view of the aft end of the apparatus during testing, allowing the influence of the tab to be seen.

5. DATA POCESSING AND ANALYSIS

The raw output voltage data acquired during testing was processed using Microsoft Excel to determine the measured magnitude and location of the lift force resulting from flow over the deflected trim tab. In addition to the measurements taken with the tab at the set tab angles, measurements were also taken without the tab in contact with the flow. This data allowed the force due to the flow acting on the two aft segments without influence from the tab to be calculated and used as a reference zero when calculating the resultant tab induced force.

The results of force variation with speed are shown here grouped by tab angles (Figure 7). It can be seen from Figure 7 that there is a regular increase of lift force with flow speed at each tab angle as expected. In particular, it is observed that 5 degree increases in tab angle from 0 to 20 degrees gave a relatively constant increase in lift force for a given flow velocity. Three data points are also shown for a tab angle of -7 degrees. The negative tab angle indicates that the tab is elevated above the horizontal. In this case a suction force was measured, as the flow did not separate from the tab until the trailing edge.

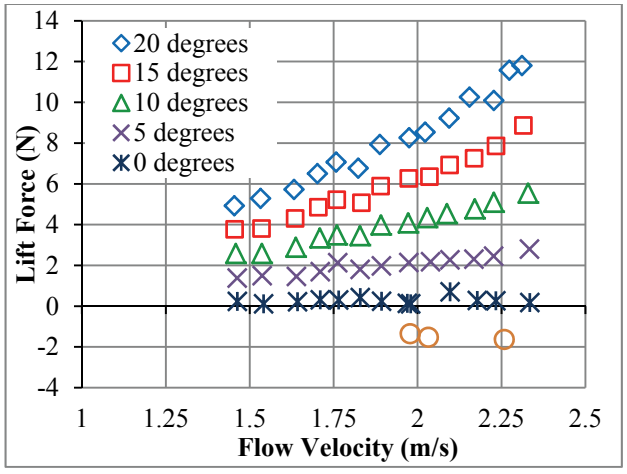

Figure 7: Magnitude of tab lift force versus flow velocity, grouped in tab angles.

There will be no lift force produced at zero flow velocity, and it is expected that the lift force will reduce to zero as the flow velocity decreased below that which was tested. The minimum *x* axis value shown on this figure is 1 m/s, and it can be seen that the trend of force magnitude against flow velocity increases parabolically from zero. This is expected as the lift force is dependent on the square of velocity as shown in Equation (10). It can be seen from the plot that the force increase appears almost linear over the tested flow velocities. This linear appearance is primarily due to the small range of velocities used in testing.

The lift coefficient data for the tab as calculated from the lift force magnitude and flow velocity (equation 10) gives a more fundamental indication of the tab performance for the test cases examined:

$$C_L = \frac{F}{\left(\frac{1}{2}\rho V^2 A\right)} \tag{10}$$

The lift coefficient plotted against tab angle is shown in Figure 8. The change in lift coefficient relative to tab angle C_L/α, is shown in Figure 8 to remain relatively constant as the tab angle increases from 0 to 20 degrees. For positive tab deflection angles the lift curve slope (C_L/α) can be estimated to be approximately 0.044 deg^{-1} from the testing results. These lift coefficient results thus indicate that the data collected was very consistent and gives a good representation of the variation in trim tab performance with changes in tab angle and flow velocity.

The force locations measured in each test case are shown in Figure 9, here shown as a function of flow speed. A negative distance value on the *y* axis indicates a distance forward of the tab hinge. We see that the lift force is located between 0.027 and 0.046 m ahead of the tab hinge, noting that the tab chord is 0.037 m. That is the force acts at a point between 0.73 and 1.24 times the tab chord ahead of the hinge.

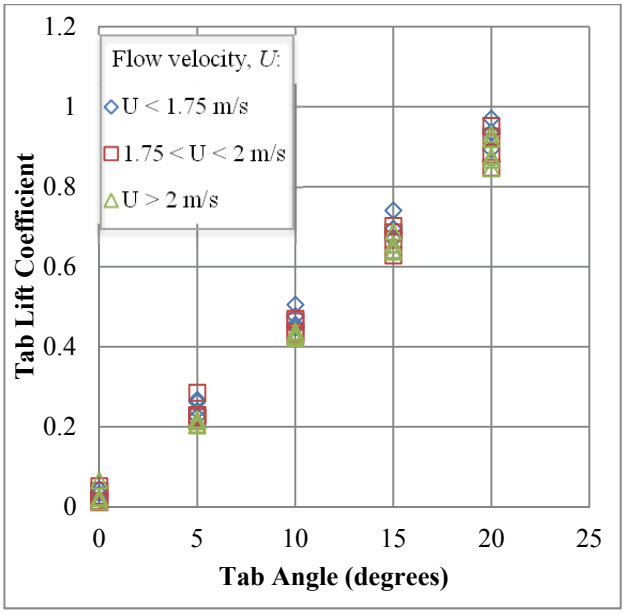

Figure 8: Tab lift coefficient versus tab angle.

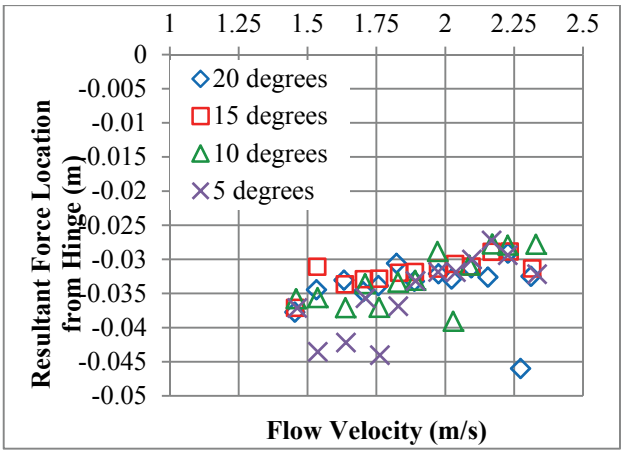

Figure 9: Effective lift force location relative to hinge (negative *y* indicates a location forward of the tab hinge, tab chord = 0.037m).

The force location was relatively constant for the test cases considered. Figure 9 shows that the force location is mainly influenced by flow speed, this mainly being attributed to a Froude number effect on the free surface flow at the stern. Flow velocities at higher Froude number are observed to cause the force centre to move aft towards the tab. It can be seen that there is a large variation in location for 5 degrees tab angle, this being due to the small forces at 5 degrees deflection making it more difficult to resolve the force location.

From these results it is clear that the distance of the force forward of the tab hinge is seen to generally reduce with an increase in flow velocity. The average distance of the force forward of the tab hinge is shown to be approximately equal to the length of the tab chord. This indicates that the tab increases the pressure on the underside of the hull at a short distance forward of the tab hinge and this pressure distribution upstream of the hinge is a very significant contributor to the total lift force. This is an important outcome as the further aft the lift force acts the greater will be the trim moment on the towing tank model or full sized vessel produced by a given total force magnitude.

6. CONCLUSIONS

The results show that the lift force produced by the stern tab increases in proportion to the square of flow velocity, as is evident in the lift coefficient data. Relatively small lift will therefore be produced at model scale for flow velocities below 1 m/s. The lift force was also seen to increase linearly with increasing tab angle as expected. Also, the lift force was found to act forward of the tab hinge for all test conditions by between 0.73 and 1.24 times the tab chord. Thus a substantial component of the total lift force is produced by the upward pressure distribution due to the deflected trim tab ahead of the tab hinge.

By determining the effect of speed and deflection on the magnitude of the lift force provided by the tab at model scale and its effective location, the tab forces acting on the towing tank model at given conditions can now be determined. This allows the force required for optimal vessel trim at various test speeds to be adjusted by the tab downward deflection, as most of these high-speed hull forms tend to adopt a bow up trim at speed if not corrected. The results obtained here can also give an indication of the structural loads induced by the use of the trim tab and of the actuation forces that can be deployed to control ship motions. This information will therefore aid in the development of active ride control systems using towing tank models. Extrapolation of trim tab data to full scale is also required, and this is likely to depend on both Froude and Reynolds numbers. Froude scaling is of course applied in any ship model testing, and so the main issue with scale up to full scale may be Reynolds scaling due to the relatively small size of the model tabs. As mentioned previously, scale up to full size may be affected by water jet intakes and boundary layer effects on the whole hull, the focus of the tests described in this paper being on local effects near the tab.

7. REFERENCES

[1] Lavroff, J., Davis, M. R., Holloway, D. S., Thomas, G., Determination of Wave Slamming Loads on High-Speed Catamarans by Hydroelastic Segmented Model Experiments, *International Journal of Maritime Engineering, Volume 153 (A3), pp 185-197,* 2011.

[2] Thomas, G., Davis, M. R., Holloway, D. S. Roberts, T. J., The Whipping Vibration of Large High-Speed Catamarans, *Transactions of the Royal Institution of Naval Architects, Volume 145 (A4), pp 13-29,* 2003.

[3] Thomas, G., Davis, M. R., Holloway, D. S., Watson, N. L., Roberts, T. J., Slamming Response of a Large High-Speed Wave-Piercer Catamaran, *Marine Technology, Volume 40 (2), pp 126–140,* 2003.

[4] Thomas, G. Davis, M. R.,Roberts, T. J., Transient Dynamic Slam Response of Large High-Speed Catamarans, *7th International Conference on Fast Sea Transportation, FAST '03,* 2003.

[5] Lavroff, J., Davis, M. R., Holloway, D. S., Thomas, G., The Vibratory Response of High Speed Catamarans to Slamming Investigated by Hydroelastic Segmented Model Experiments,*Transactions of the Royal Institution of Naval Architects, Volume 151 pp 1–12,* 2010.

[6] Lavroff, J., The Slamming and Whipping Vibratory Response of a Hydroelastic Segmented Catamaran Model, *PhD Thesis, University of Tasmania,* 2009.

[7] Thomas G., Winkler S,. Davis M. R., Holloway D. S., Matsubara S., Lavroff J., French B., Slam Events of High-Speed Catamarans in Irregular

Waves, *Journal of Marine Science and Technology, Volume 16*, *pp 8-21,* 2010.

[8] Davis,M. R.,Watson, N. L., Holloway, D. S., Measurement of Response Amplitude Operators for an 86 m High-Speed Catamaran,*Journal of Ship Research, Volume 49, pp 121-143,* 2005.

[9] Jacobi, G., High-speed Catamaran Motion Response and Slamming Behaviour During Full Scale Trials,*Diploma of Engineering (Naval Architecture) Masters Thesis, University Rostock,*2011.

[10] Davis, M. R., Holloway, D. S., Motion and Passenger Discomfort on High Speed Catamarans in Oblique Seas, *International Shipbuilding Progress*, *Volume 50, (4) pp 333-370,* 2003.

[11] Holloway, D. S., Davis,M. R., Ship Motion Using a High Froude Number Time Domain Strip Theory,*Journal of Ship Research, Volume 50, pp 15-30,* 2006.

[12] I. T. T. Conference, ITTC - Recomended Procedures and Guidelines: Model Manufacture - Ship Models,*International Towing Tank Conference*, *pp 4,* 2008.

[13] Davis, M. R., The Fluid Dynamics of Water Jet Propulsion Units,*Ausmarine '96,pp 1-19,*1996.

